UNCLASSIFIED

NACA

RESEARCH MEMORANDUM

INVESTIGATION OF A HIGH-PRESSURE-RATIO EIGHT-STAGE

AXIAL-FLOW RESEARCH COMPRESSOR WITH TWO

TRANSONIC INLET STAGES

VI - OVER-ALL PERFORMANCE, ROTATING STALL, AND BLADE

VIBRATION AT LOW AND INTERMEDIATE COMPRESSOR SPEEDS

By Raymond M. Standahar, Morgan P. Hanson, and Richard P. Geye

Lewis Flight Propulsion Laboratory
Cleveland, Ohio

CLASSIFICATION CHANGED

UNCLASSIFIED

NATIONAL ADVISORY COMMITTEE
FOR AERONAUTICS
WASHINGTON
November 1, 1955

UNCLASSIFIED

3844

T-CC-1

NATIONAL ADVISORY COMMITTEE FOR AERONAUTICS

RESEARCH MEMORANDUM

INVESTIGATION OF A HIGH-PRESSURE-RATIO EIGHT-STAGE AXIAL-FLOW

RESEARCH COMPRESSOR WITH TWO TRANSONIC INLET STAGES

VI - OVER-ALL PERFORMANCE, ROTATING STALL, AND BLADE

VIBRATION AT LOW AND INTERMEDIATE COMPRESSOR SPEEDS

By Raymond M. Standahar, Morgan P. Hanson, and Richard P. Geye

SUMMARY

An investigation to determine the over-all performance of the modified eight-stage axial-flow compressor with new fourth-stage stator blades was conducted as part of the study of the problems encountered in a high-pressure-ratio axial-flow compressor with transonic inlet stages. The performance of the compressor was determined over a range of weight flows at equivalent speeds from 30 to 100 percent of design speed. The surge, rotating-stall, and blade vibration characteristics were determined at low and intermediate speeds. The maximum total-pressure ratio obtained at design speed was 10.7 at an equivalent weight flow of 70.5 pounds per second (29.7 lb/(sec)(sq ft of frontal area)) with an adiabatic efficiency of 0.82. A maximum equivalent weight flow of approximately 72.5 pounds per second (30.6 lb/(sec)(sq ft of frontal area)) was obtained at design speed.

Rotating stall was present up to equivalent speeds of approximately 73 percent of design speed. The stall patterns obtained were of either the three- or four-zone partial-span type. Rotating stall excited resonant vibration in the compressor blading. The resulting blade stresses were determined by the use of resistance-type strain gages mounted near the top of the blade-base fillet on two blades of each blade row. The peak vibratory stresses in the first- and second-stage stator blades were ±45,500 pounds per square inch at 6350 rpm and ±59,500 pounds per square inch at 8250 rpm, respectively. In the rotor blades, the highest vibratory stress was ±17,700 pounds per square inch occurring in the fourth stage at 7900 rpm.

INTRODUCTION

In the study of the design and off-design performance problems of a high-mass-flow, high-pressure-ratio, multistage compressor, an eight-stage axial-flow compressor having two transonic inlet stages was designed, fabricated, and tested at the NACA Lewis laboratory. Reference 1 presents a detailed study of the aerodynamic design and over-all performance data of this compressor. During the course of this study, several modifications were incorporated in the compressor in an attempt to improve the mechanical characteristics of the blading and the aerodynamic performance at high speeds. These modifications included tapering the internal casing diameter from 20 inches at the entrance of the seventh stage to 20.86 inches at the first-stage entrance, reducing the rate of change of hub curvature through the first and second stage to a minimum allowed by stress considerations, and enlarging the base fillets to reduce the possibility of blade failure (ref. 2).

During the over-all performance tests of the modified compressor, fatigue cracks were detected in the fourth stator row, and the tests were stopped before the performance in the intermediate speed range could be determined. A new set of fourth-stage stator blades with a larger base diameter and a larger root fillet were then installed, and the tests continued.

This report presents the over-all performance on the basis of total-pressure ratio and adiabatic temperature-rise efficiency plotted against inlet equivalent weight flow for a range of speeds from 30 to 100 percent of design. The rotating-stall regions are also indicated on the over-all performance map. Critical-speed diagrams are presented for the rotor and stator blades to indicate the rotating-stall excitation. An equilibrium operating line is superimposed on the compressor performance map to indicate the part-speed problems associated with installation of this compressor in a turbojet engine.

SYMBOLS

The following symbols are used in this report:

f_s frequency with which stall regions pass anemometer probe

h rotative speed of propagating stall region, rps

N rotor speed, rpm

P total pressure, lb/sq ft abs

Re Reynolds number relative to tip of first rotor

T   total temperature, $°F$

w   weight flow, lb/sec

δ ratio of inlet total pressure to NACA standard sea-level pressure of 2116 lb/sq ft

η_{ad} adiabatic temperature-rise efficiency

θ ratio of inlet total temperature to NACA standard sea-level temperature of $518.7°$ R

λ number of stall zones

Subscripts:

0   inlet depression-tank station

20   discharge measuring station

Superscript:

'   relative to rotor blading

APPARATUS

Compressor

The compressor used for this investigation was a 20.856-inch inlet tip diameter, eight-stage axial-flow research compressor having two transonic inlet stages. A cross-sectional view of the compressor, the inlet bellmouth nozzle, and the discharge collector is shown in figure 1. The original compressor was designed for an over-all total-pressure ratio of 10.26 at an equivalent weight flow of 72.4 pounds per second (ref. 1). A description of the various modifications of the compressor is presented in reference 2, and a preliminary analysis of the over-all performance is given in reference 3. Before running the tests reported herein, the fourth row of stator blades was replaced with blades having larger root fillets and larger base diameters because of the fatigue cracks that developed during the tests reported in reference 3.

Installation

The compressor was driven by a 15,000-horsepower, variable-frequency electric motor. The speed was maintained constant by an electronic control and was measured by an electric chronometric tachometer. Air entered the compressor through a submerged thin-plate orifice, a butterfly

inlet throttle for controlling inlet pressure, and a depression tank 6 feet in diameter and approximately 10 feet long. Screens in the depression tank and a bellmouth nozzle faired into the compressor inlet were used to obtain a uniform distribution of air entering the compressor. Air was discharged from the compressor into a collector connected to the laboratory altitude exhaust system. Air weight flow was controlled by a butterfly valve located in the exhaust ducting.

Instrumentation

The axial locations of the instrument-measuring stations are shown in figure 1. The inlet depression-tank station and the compressor discharge had axial locations that were in accordance with reference 4. Radial distributions of outlet total temperature and total pressure were obtained from multiple-probe rakes located at the area centers of equal annular areas. The instruments used at each station and the method of measurement are the same as given in reference 3.

The vibratory stress of two blades in each of the rotor and stator blade rows was measured by means of two resistance-wire strain gages cemented to opposite sides of the blades at the thickest base section. The gages were connected in a bridge circuit, and the output was recorded on an oscillograph. A detailed description of the strain-gage instrumentation is given in reference 5.

The constant-temperature hot-wire system was used to detect rotating stall (ref. 6). The hot-wire filaments were 0.001 inch in diameter, 0.1 inch long, and positioned in a radial direction. The probes were located after the first and third rotors and were mounted in actuators allowing a radial traverse. The hot-wire and strain-gage signals were recorded on a multiple-channel oscillograph.

The accuracy of measurement is estimated to be within the following limits: temperature, $\pm 1.0^\circ$ F; pressure, ± 0.05 inch of mercury; weight flow, ± 1.5 percent; and speed, ± 0.3 percent.

PROCEDURE

The compressor was operated at equivalent speeds corresponding to 72.5, 75, 80, 90, and 100 percent of design speed at air flows ranging from maximum flow to a flow at which surge or stall occurred. In these tests, an audible surge occurred at minimum flow at each speed tested. This line will be called the surge-limit line. The surge line was further defined in the region of the knee by taking additional data at 74 and 77.5 percent of design speed. At 30, 50, 60, and 70 percent of

3844

design speed, a few data points were taken to check the data of reference 3, but no surge points were taken in order to conserve the hot-wire anemometers installed in the compressor. An oscillograph recorded the stress and vibration data.

In order to make a complete investigation of the rotor and stator blade vibration, the strain-gage signals at all rotor speeds had to be observed. Visual observations were made on both an oscilloscope and the scanning system of the oscillograph. The strain-gage signal was recorded wherever peak vibrations were observed. Generally, the recordings were made during slow accelerations or decelerations to avoid sustained operation at resonance conditions. By this method of recording, off-resonance measurements of the vibration were also possible. The magnitude of the vibration, in terms of stress, and the frequency of the vibration were determined from the recorded signals. The inlet pressure was varied to maintain approximately a constant Reynolds number (based on the blade chord at the tip of the first rotor and the air velocities relative to the tip of the first rotor) of 1,000,000 at all speeds except 30 percent of design speed. Refrigerated inlet air was used at all speeds to limit the outlet temperature and the mechanical speed of the compressor for a given equivalent speed. A continuous check was kept on the blade vibration so that operation in regions of high vibratory stress could be kept to a minimum.

Radial surveys with the hot-wire anemometer were taken at operating points where rotating stall was present. The number of stall zones in each stall pattern was determined by the methods outlined in reference 7. For each flow point, the calculated discharge total pressure was obtained by the method presented in reference 4.

RESULTS AND DISCUSSION

Over-All Compressor Performance

Total-pressure ratio and adiabatic efficiency. - The over-all performance characteristics of the compressor are presented as a plot of total-pressure ratio as a function of equivalent weight flow for various values of speed with the contours of constant adiabatic efficiency (fig. 2). At design speed, a maximum total-pressure ratio of 10.7 was obtained at an equivalent weight flow of 70.5 pounds per second (29.7 lb/(sec)(sq ft of frontal area)) with an efficiency of 0.82. A peak efficiency of 0.83 was obtained at total-pressure ratios ranging from about 9.3 to 10.3 and a maximum weight flow of approximately 72.5 pounds per second (30.6 lb/(sec)(sq ft of frontal area)) was obtained. The over-all performance curve taken from reference 3 is also presented in figure 2. At 90 and 100 percent of design speed, the surge pressure ratio is slightly lower than that of reference 3. The over-all adiabatic

temperature-rise efficiency is plotted as a function of equivalent
weight flow in figure 3, and the over-all efficiency curve of reference
3 is also presented. The efficiency reached a maximum value of 0.84 at
90 percent of design speed and dropped to 0.83 at design speed. This
is approximately a one-point drop in peak efficiency from that obtained
in reference 3. Although this difference in peak efficiency is within
experimental limits, it is believed that replacing the fourth-stage sta-
tor blades with the new set of blades having larger root fillets may
have been a contributing factor to this difference.

The compressor-surge line can be approximated by two straight
lines, one running from 30 to 60 percent of design speed and the other
from 75 to 100 percent of speed and connected by a smooth curve. There
is no sharp "knee" in this surge line, and as shown by figure 2, the
greatest change in slope occurs in the speed range where the compressor
moves out of rotating stall.

To indicate the part-speed problems associated with installation
of this compressor in a turbojet engine, an equilibrium operating line
is superimposed on the compressor map (fig. 4) by using the approximate
method of reference 8. In order to obtain an operating line, the fol-
lowing engine operating conditions at design speed were selected for
sea-level static conditions: compressor pressure ratio, 9.0; ratio of
turbine- to compressor-inlet temperature, 4.0; and turbine efficiency,
0.85. At compressor pressure ratios less than 9.0, the turbine operat-
ing line used was for a multistage turbine (see ref. 8) with a constant
efficiency of 0.85. With a fixed exhaust-nozzle area, the operating
line moved into the surge region at approximately 76 percent of equiva-
lent design speed. It was necessary to increase the nozzle area by 10
percent before the operating-line would stay in the region of stable
operation over the entire range. Actually this increase would not be
enough to allow any margin for acceleration. Consequently, a larger
exhaust-nozzle area would be necessary, or some other method such as
bleed would have to be used to obtain acceleration margin. This re-
sult indicates that this type of high-pressure-ratio compressor will
require some variable-geometry scheme for acceleration purposes.

Rotating stall. - The presence of rotating stall in the compressor
annulus was indicated by means of a hot-wire anemometer. The stall ex-
tended axially through the compressor and propagated in the direction
of rotation of the compressor. The flow disturbance due to rotating
stall was confined to the outer half of the annulus with maximum strength
at the tip. Three stall zones rotating at 45 percent of rotor speed and
four stall zones rotating at 51 to 54 percent of rotor speed were pre-
dominant during part-speed operation (fig. 4). The lines which separate
the operating regions for each number of stall zones must be considered
approximate, as the stall patterns are intermittent near the line of
transformation.

Only two major stall patterns of three or four zones could be located in the compressor during these tests. There was no rotating-stall indication near the surge line at 74 percent of design speed, but a three-zone stall was encountered as the speed was reduced to 72.5 percent speed. As the weight flow was increased at 72.5 percent speed, the stall pattern became progressively weaker, but it was not possible to get the machine completely out of stall. The first noticeable four-zone stall region appeared at 67 percent speed, but it was unstable and alternated with a three-zone stall. A strong four-zone stall region was evident only at speeds lower than approximately 65 percent of design speed, and then only in a narrow band near the surge line.

A plot of the absolute rotating-stall frequency against actual rotor speed is shown in figure 5. The rotating-stall frequency varies as a linear function of the rotor speed. Changes in inlet temperature have no effect on stall-propagation rate at a given mechanical speed, if the number of stall zones remains the same. The ratio of stall speed h to compressor speed N remains constant as inlet temperature is varied. For a given operating point (a particular value of corrected speed $N/\sqrt{\theta}$ and corrected weight flow $w\sqrt{\theta}/\delta$), the stall pattern is generally fixed. If the mechanical speed is changed to accommodate inlet-temperature changes so that the corrected speed is constant, the stall frequency will change with the changes in inlet temperature. The four-zone stall existed over a range of speeds from 3250 to 7950 rpm (24 to 60 percent of rated mechanical speed) and the three stall zones over a range from 6000 to 8800 (45 to 66 percent of rated mechanical speed). Figure 5 shows the mechanical-speed range over which rotating stall was observed during the investigation. Rotating stall can excite compressor blading to resonant vibration, which may result in blade failure (ref. 9). Therefore, a study was made to determine at which compressor speeds resonant vibration of blades excited by rotating stall was likely to occur.

Stator Blade Vibration

Since rotating-stall frequency varies linearly with rotor speed and the stator blade natural frequency remains constant, resonance between the two frequencies can be studied by means of a critical speed diagram (fig. 6). Since the flow fluctuations of rotating stall are not simply sinusoidal, the harmonics of the flow fluctuations may contain sufficient energy to induce appreciable vibrations and therefore are included in the diagram. Another possible source of stator blade excitation (not shown on the diagram) is the rotor blade wakes.

Numerous resonance speeds become apparent from the critical-speed diagram. The significant stator blade vibrations occurred in the first and second stages with the blade vibrating in the fundamental bending

mode. The remaining stages experienced only minor vibrations. The
critical-speed diagram also indicates the possible excitation which
caused fatigue cracks in the original fourth-row stator blades.

Figure 7 shows the amplitude of the blade vibration of the first
three stages in terms of vibratory stress in the speed range of the com-
pressor where rotating stall occurred. In the first stage a single peak
stress of ±45,600 pounds per square inch at 6350 rpm was due to the
blade frequency's being in resonance with the fundamental of the four-
zone-stall pattern. In the second stage two peaks were observed cor-
responding to resonance with the second harmonic of the four-zone stall
at 5300 rpm and the second harmonic of the three-zone stall at 8250 rpm,
with a stress amplitude of ±12,500 and ±59,500 pounds per square inch,
respectively. In the third stage three peaks were observed. Two of the
stress peaks were induced by the third harmonic of either the four- or
three-zone rotating-stall patterns. These stress peaks occurred at 4600
and 7200 rpm with stress amplitudes of ±12,000 and ±17,000 pounds per
square inch, respectively. The third peak of ±21,000 pounds per square
inch at 8625 rpm does not appear as a resonance point in figure 6. How-
ever, an examination of the rotating-stall pattern revealed a noticeable
difference in signal amplitude between zones. Basically, a three-zone
stall was present but every other zone had a greater signal amplitude
than the preceding or succeeding one (fig. 8). Consequently, the ex-
citing frequency established itself as one-half the fundamental three-
stall frequency or approximately 98 cycles per second at 8625 rpm. The
fifth harmonic of the one-half frequency (i.e., 98 cps) is in resonance
with the third-stage blade natural frequency.

It is interesting to note in figure 7 that minor stress peaks occur
in the vibratory stress at rotor speeds not indicated as critical speeds
in figure 6. A source of excitation is evidently present and could be a
rotating-stall component that was not observed from the hot-wire anemom-
eter. However, the stress levels are low and insignifcant from a mechan-
ical consideration.

A vibration of interest but not shown in the stress plot (fig. 7)
was that of a second-bending-mode vibration in the second-stage blade.
The frequency of the vibration was 2240 cycles per second occurring at
a rotor speed of 5840 rpm. The resonance condition was the result of
the second bending frequency being in resonance with the fundamental of
the second-stage rotor blade wake frequency. The vibratory stress was
found to be low (±7550 psi, as measured at the blade base). The low-
level vibration is an indication of the low exciting energy of blade
wakes and contrasts the generally high energy of rotating stall. Fig-
ure 8 presents an oscillogram of hot-wire anemometer and strain-gage
signals of the third-stage stator blade vibration at 8625 rpm (fig. 7).

Rotor Blade Vibration

In considering rotating stall as a source of vibration excitation in the rotor blades, the rotating-stall frequency relative to the rotor must be determined. Since the rotating-stall zones are propagating in the same direction as compressor rotation, the frequency f'_s relative to the blades can be computed by

$$f'_s = \frac{N\lambda}{60} - f_s$$

where

N   rotor speed, rpm

λ number of stall zones

Knowing the rotating-stall frequency relative to the rotor blades, a critical-speed diagram of the rotor blades can be constructed similar to that of the stator blades (fig. 9). Since the rotor blades are subjected to centrifugal force, the natural frequency increases somewhat with the rotor speed. Again, the stall and blade frequencies intersect showing possible critical speeds. Whenever the blade frequency is an exact multiple of the rotor speed, resonance can occur if a stationary excitation such as a strut wake is present. The multiple is commonly referred to as an order number. To avoid confusion, only the second- and sixth-order lines are shown in figure 9.

Observation of the critical-speed diagram for the rotor blades indicates that several critical speeds occur. The blade-vibration data obtained is shown in figure 10. In contrast to the stator response, no significant vibrations were observed in the first and second stages. Low-level vibration (under 10,000 psi) was experienced throughout the speed range, but minor peaks were evident at stall-zone frequency resonance points shown in figure 9. The first- and second-stage rotor blades are somewhat stiffer than the stator blades and are consequently less subject to high vibratory stresses.

The third-stage vibration is seen to be excited by the third harmonic of both the three- and four-zone rotating stall and the fourth harmonic of the four-zone rotating stall. The resulting low vibratory stress is possibly due to the low-energy content of the third and fourth harmonics of either the three- or four-zone rotating stall. This is logical since the third and fourth harmonics were likewise weak in exciting stator blade vibration.

The highest vibration in the rotor blades was observed in the fourth stage where the maximum vibratory stress was ±17,700 pounds per square

inch occurring at 7900 rpm (fig. 10). From figure 9 it is difficult to
ascertain the source of the excitation because of the close proximity
of the sixth order and the third harmonic of the four stall zones. How-
ever, an analysis of a particular vibration measurement reveals that the
sixth order was equal to the blade frequency (790 cps), whereas the
relative rotating-stall frequency was only 775 cps. The origin of a
sixth-order excitation does not appear evident. Since no sixth-order
excitation occurred in any of the preceding stages, it is obviously
limited to the particular speed (7900 rpm). The remaining fourth-stage
blade vibrations were definitely due to rotating-stall excitation, but
they were low in amplitude. The low-level vibration was probably due
to the presumably low-energy harmonics of the flow fluctuations of ro-
tating stall as experienced in the third-stage excitation. The possi-
bility of greater damping in the rotor cannot be discounted. The
rotor blades were loose in their mounts, and this looseness could in-
crease the damping at part speed operation. The stator blades, on the
other hand, were tight.

SUMMARY OF RESULTS

The following results were obtained during the investigation of
rotating-stall and blade-vibration characteristics of the modified
eight-stage axial-flow compressor.

1. The maximum total-pressure ratio obtained at design speed was
10.7 at an equivalent weight flow of 70.5 pounds per second with an
adiabatic efficiency of 0.82.

2. A peak efficiency of 0.83 was obtained at design speed for
values of total-pressure ratio varying from about 9.3 to 10.3.

3. A maximum equivalent weight flow of approximately 72.5 pounds
per second (30.6 lb/(sec)(sq ft of frontal area)) was obtained at de-
sign speed.

4. The presence of rotating-stall patterns was indicated up to
equivalent speeds of approximately 73 percent of design speed. The
patterns obtained were of either the three- or four-zone type.

5. The peak vibratory stress in the first- and second-stage stator
blades were ±45,500 pounds per square inch at 6350 rpm and ±59,500
pounds per square inch at 8250 rpm, respectively. These high stresses
were the result of resonance with rotating-stall frequencies. The
highest vibratory stress in the rotor blades (±17,700 psi) occurred
in the fourth-stage rotor at 7900 rpm.

Lewis Flight Propulsion Laboratory
      National Advisory Committee for Aeronautics
            Cleveland, Ohio, September 14, 1955

REFERENCES

1. Voit, Charles H.: Investigation of a High-Pressure-Ratio Eight-Stage Axial-Flow Research Compressor with Two Transonic Inlet Stages. I - Aerodynamic Design. NACA RM E53I24, 1953.

2. Geye, Richard P., and Voit, Charles H.: Investigation of a High-Pressure-Ratio Eight-Stage Axial-Flow Research Compressor with Two Transonic Inlet Stages. IV - Modification of Aerodynamic Design and Prediction of Performance. NACA RM E55B28, 1955.

3. Standahar, Raymond M., and Geye, Richard P.: Investigation of a High-Pressure-Ratio Eight-Stage Axial-Flow Research Compressor with Two Transonic Inlet Stages. V - Preliminary Analysis of Over-All Performance of Modified Compressor. NACA RM E55A03, 1955.

4. NACA Subcommittee on Compressors: Standard Procedures for Rating and Testing Multistage Axial-Flow Compressors. NACA TN 1138, 1946.

5. Meyer, André J., Jr., and Calvert, Howard F.: Vibration Survey of Blades in 10-Stage Axial-Flow Compressor. II - Dynamic Investigation. NACA RM E8J22a, 1949.

6. Shepard, Charles E.: A Self-Excited, Alternating-Current, Constant-Temperature Hot-Wire Anemometer. NACA TN 3406, 1955.

7. Huppert, Merle C.: Preliminary Investigation of Flow Fluctuations During Surge and Blade Row Stall in Axial-Flow Compressors. NACA RM E52E28, 1952.

8. Huppert, Merle C.: Approximate Method for Determining Equilibrium Operation of Compressor Component of Turbojet Engine. NACA TN 3517, 1955.

9. Huppert, Merle C., Johnson, Donald F., and Costilow, Eleanor L.: Preliminary Investigation of Compressor Blade Vibration Excited by Rotating Stall. NACA RM E52J15, 1952.
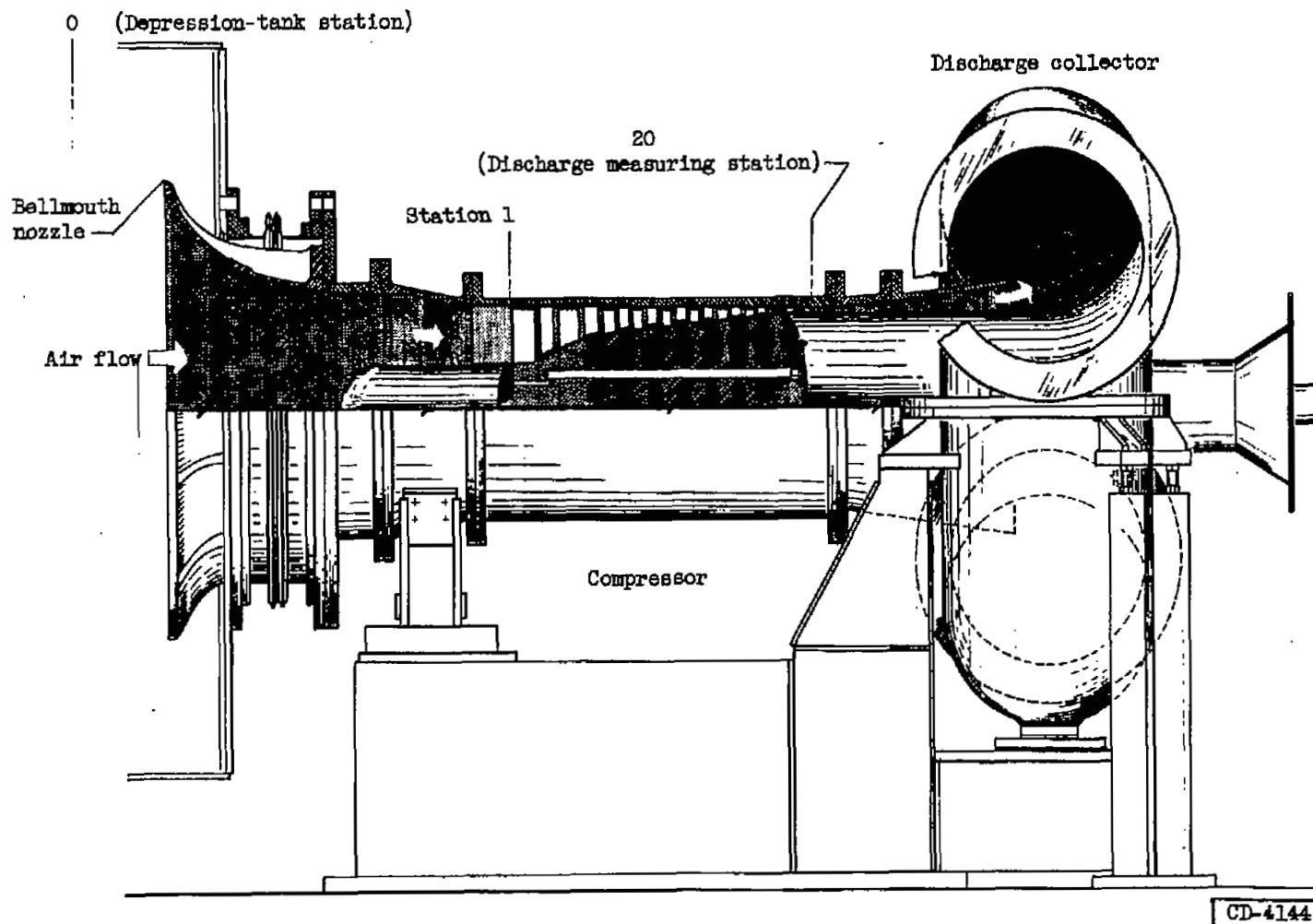
3844

GU-2 back

Figure 1. - Cross-sectional view of eight-stage axial-flow compressor, inlet bellmouth nozzle, and discharge collector.
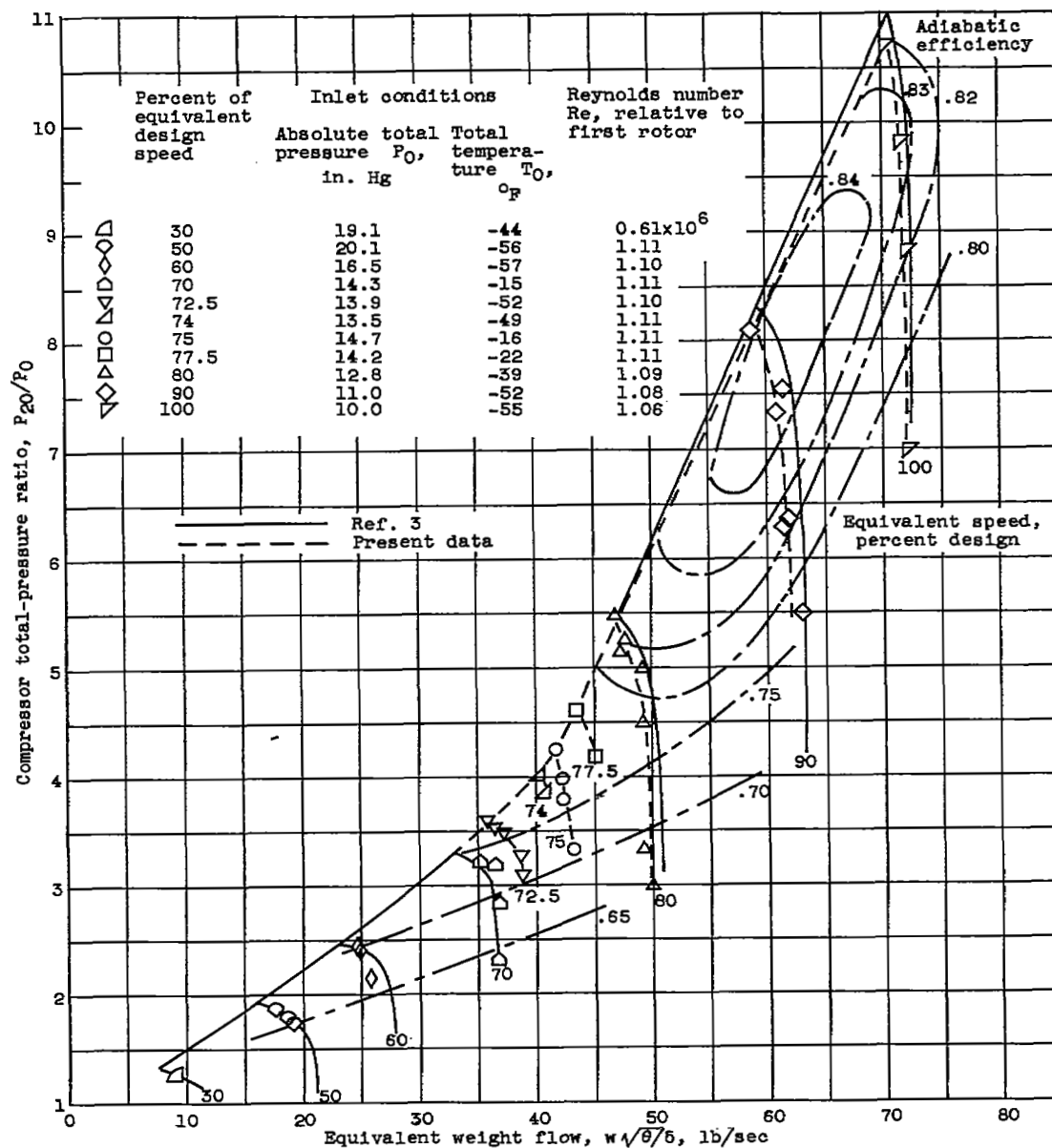
Figure 2. – Over-all performance characteristics of modified eight-stage axial-flow compressor.
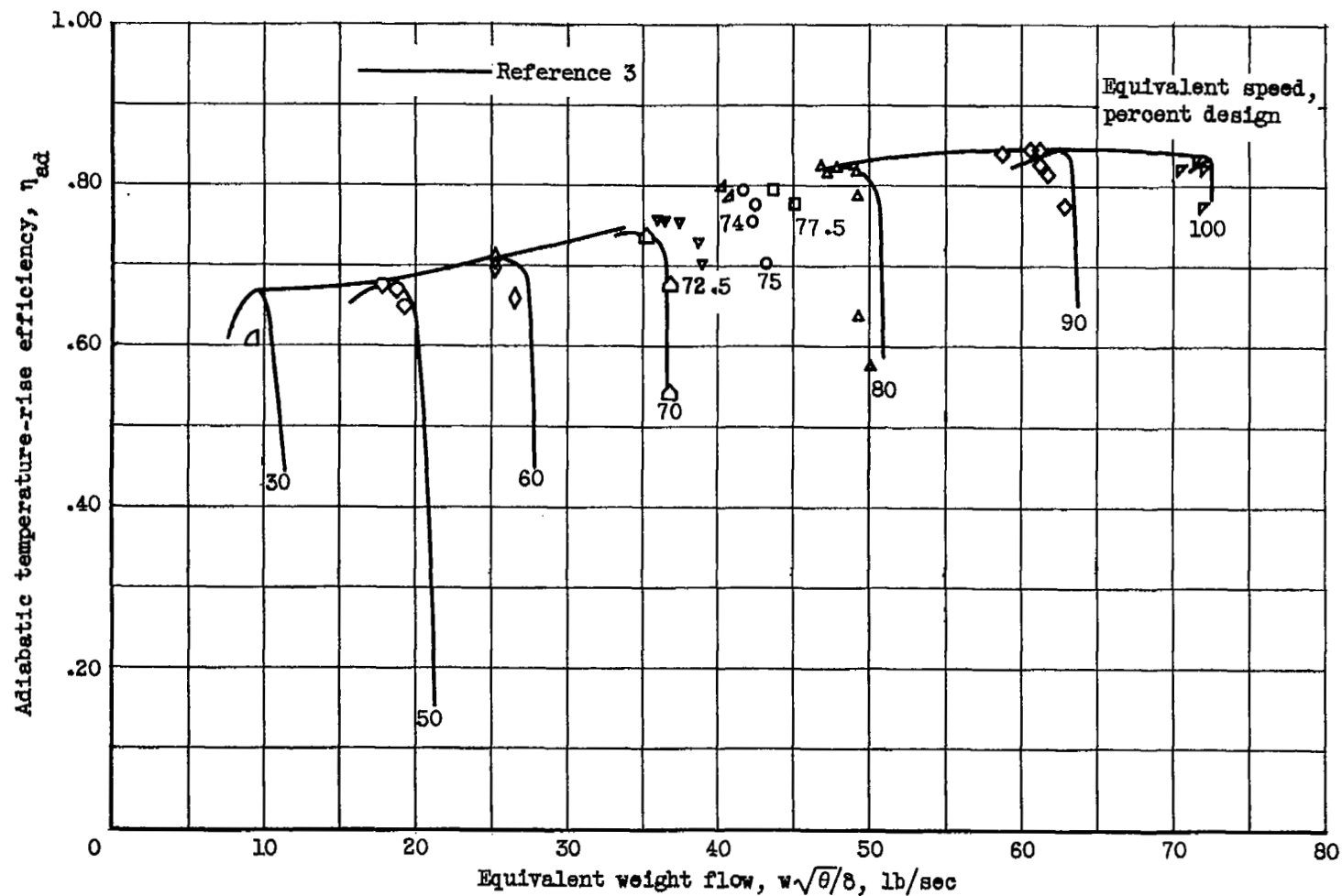
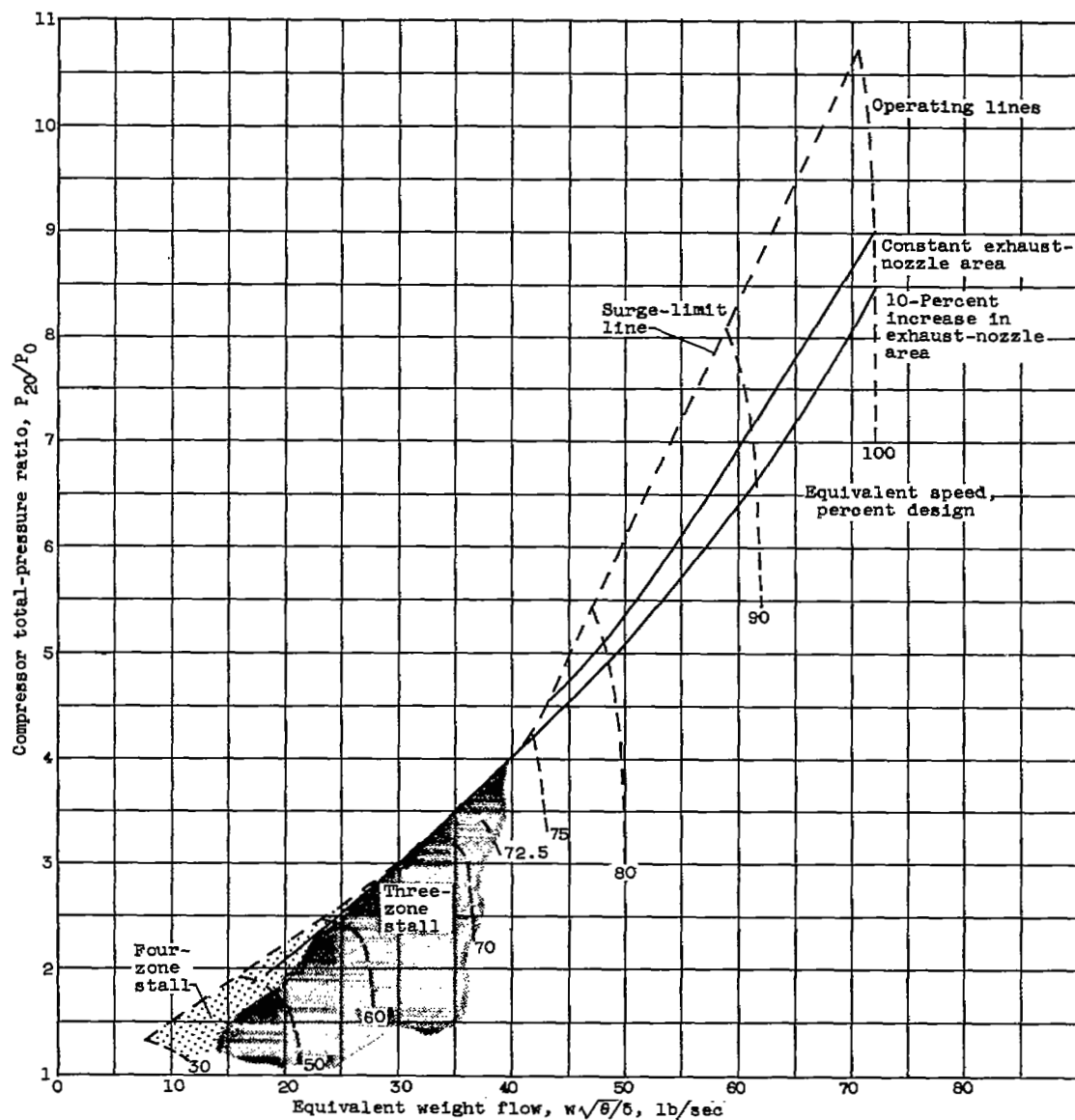Figure 3. - Variation of adiabatic temperature-rise efficiency with speed and weight flow.

3844

Figure 4. - Over-all compressor performance map showing typical equilibrium operating line and conditions at which rotating stall occurred.
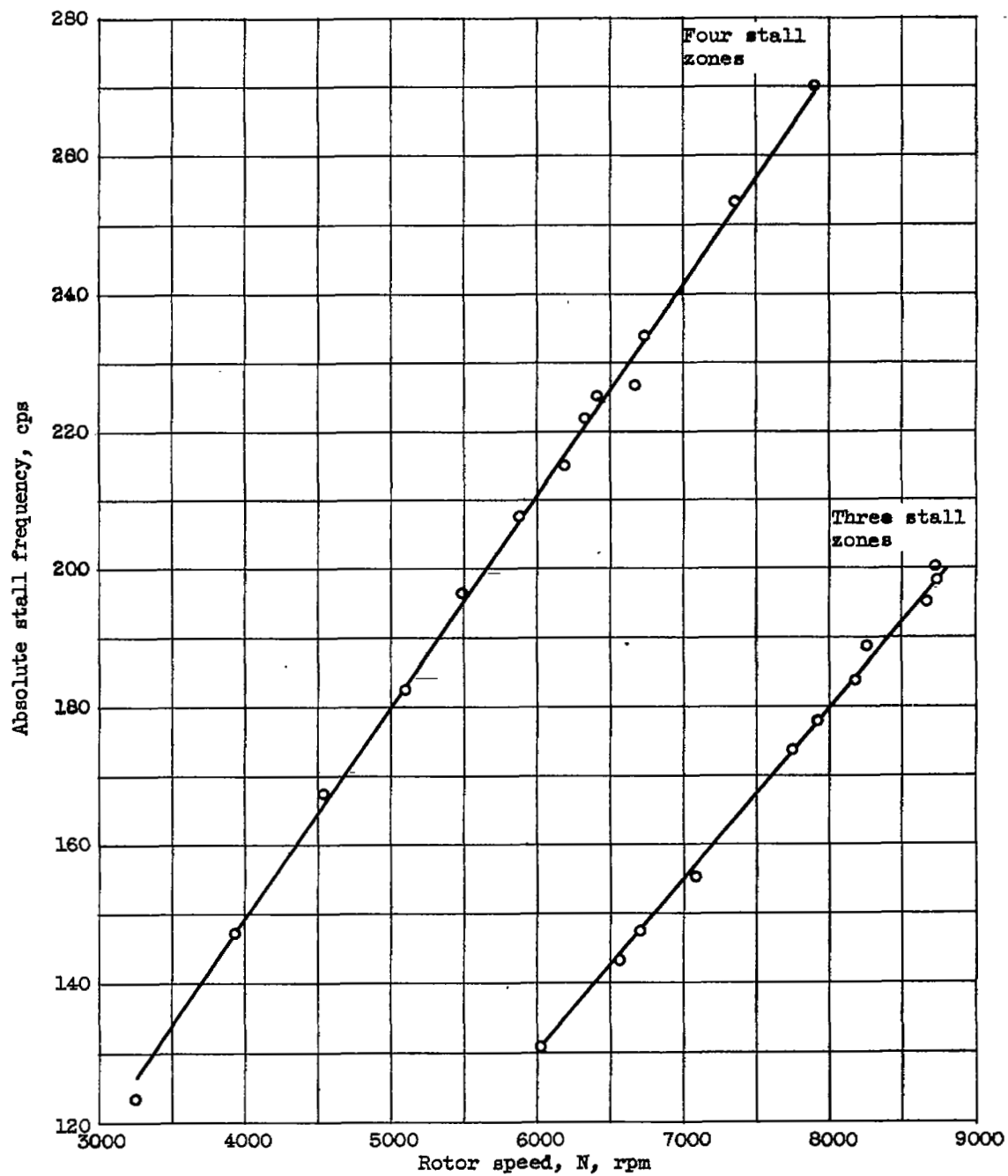
Figure 5. - Absolute stall frequency as a function of rotor speed.
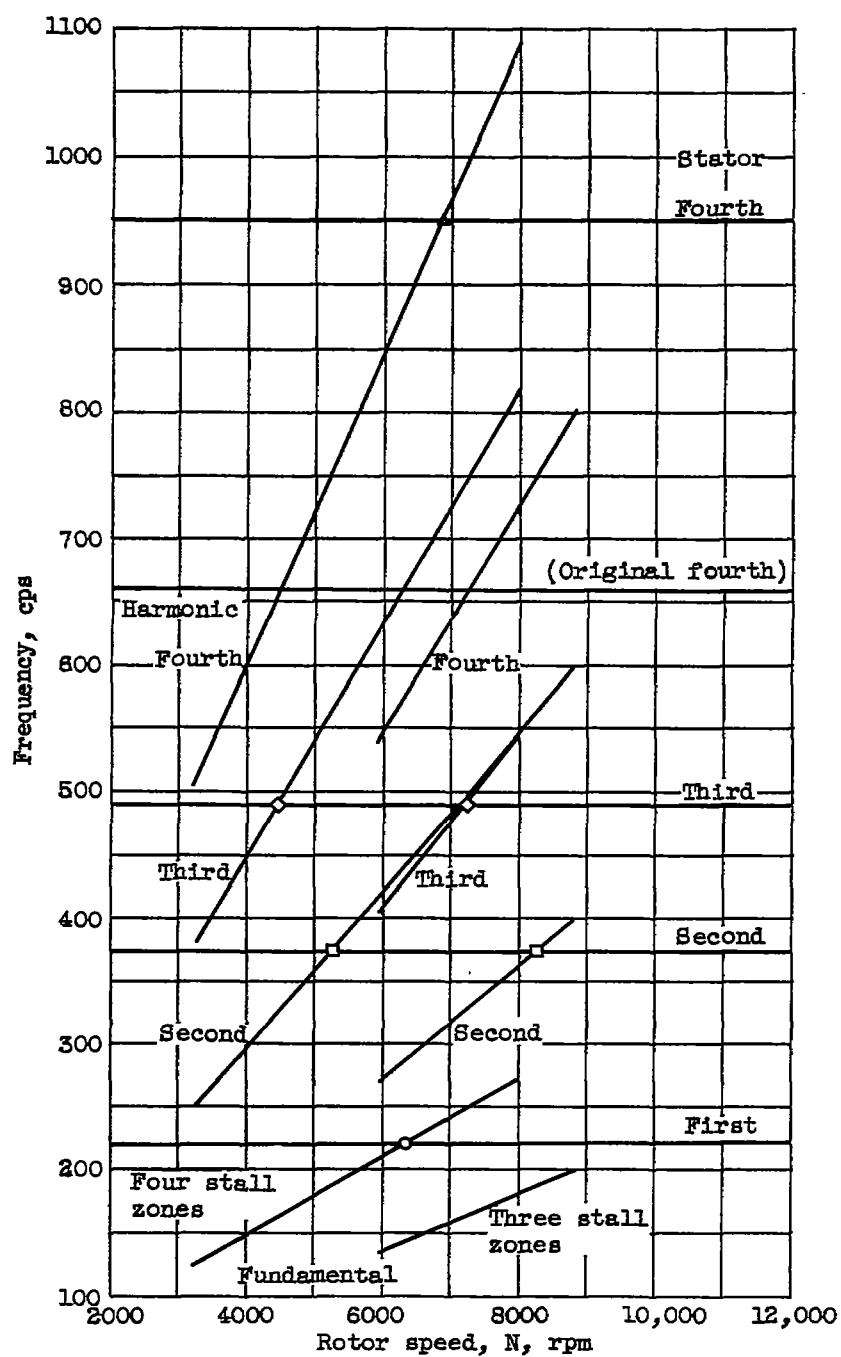
Figure 6. - Critical-speed diagram of stator blades
  indicating rotating-stall excitation. Stress encoun-
  tered at data points shown on figure 7.
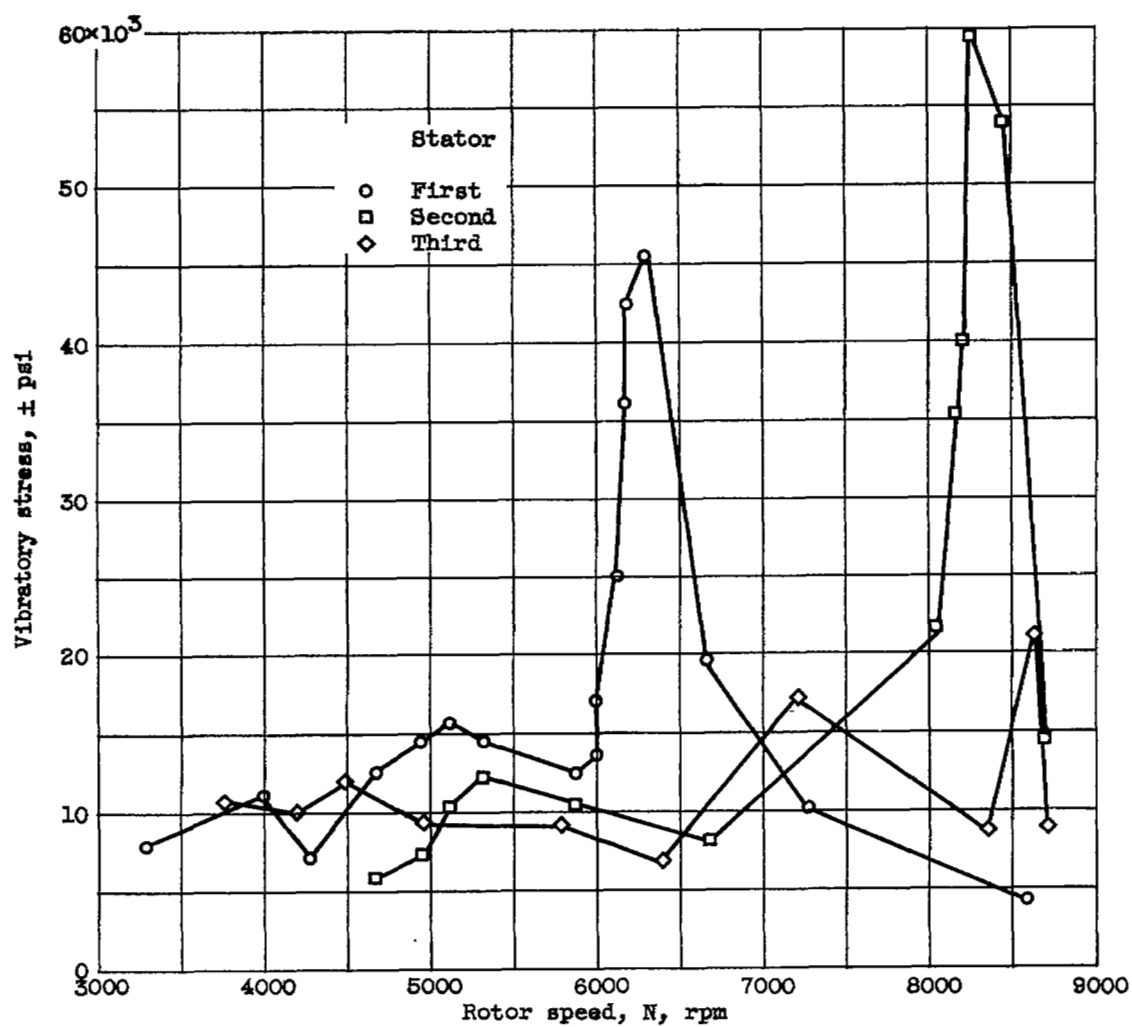
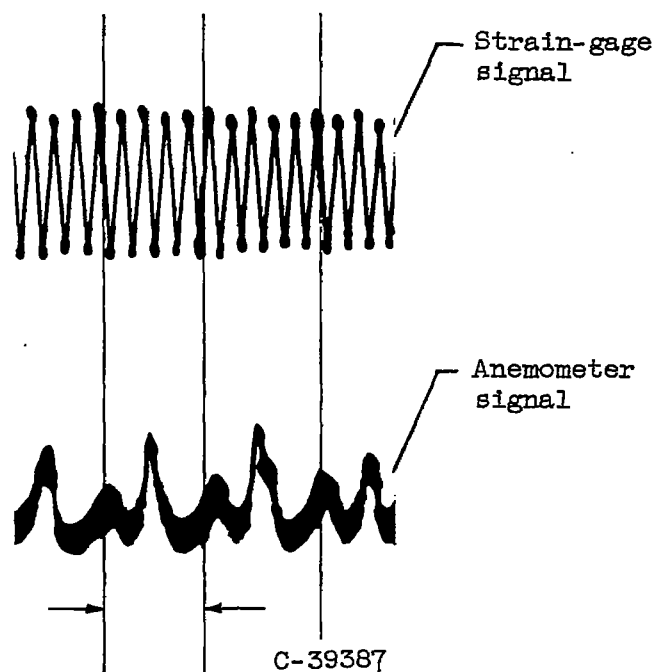Figure 7. - Variation of stator blade vibration with rotor speed.

Figure 8. - Oscillogram of hot-wire anemometer
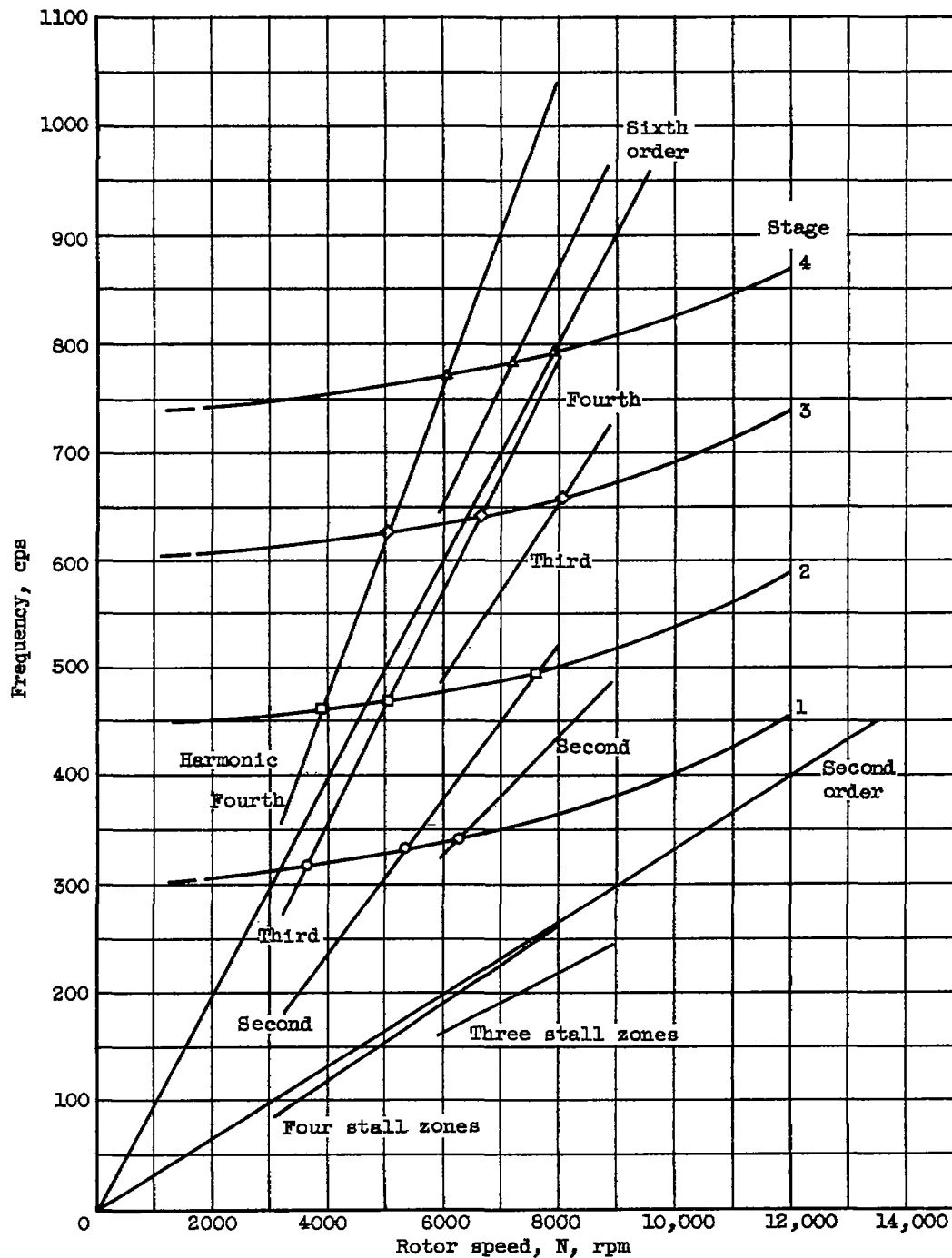   and strain-gage signals (third-stage vibration,
    8625 rpm, fig. 7).

Figure 9. - Critical-speed diagram of rotor blades indicating rotating
stall and order excitation. Stress encountered at data points shown
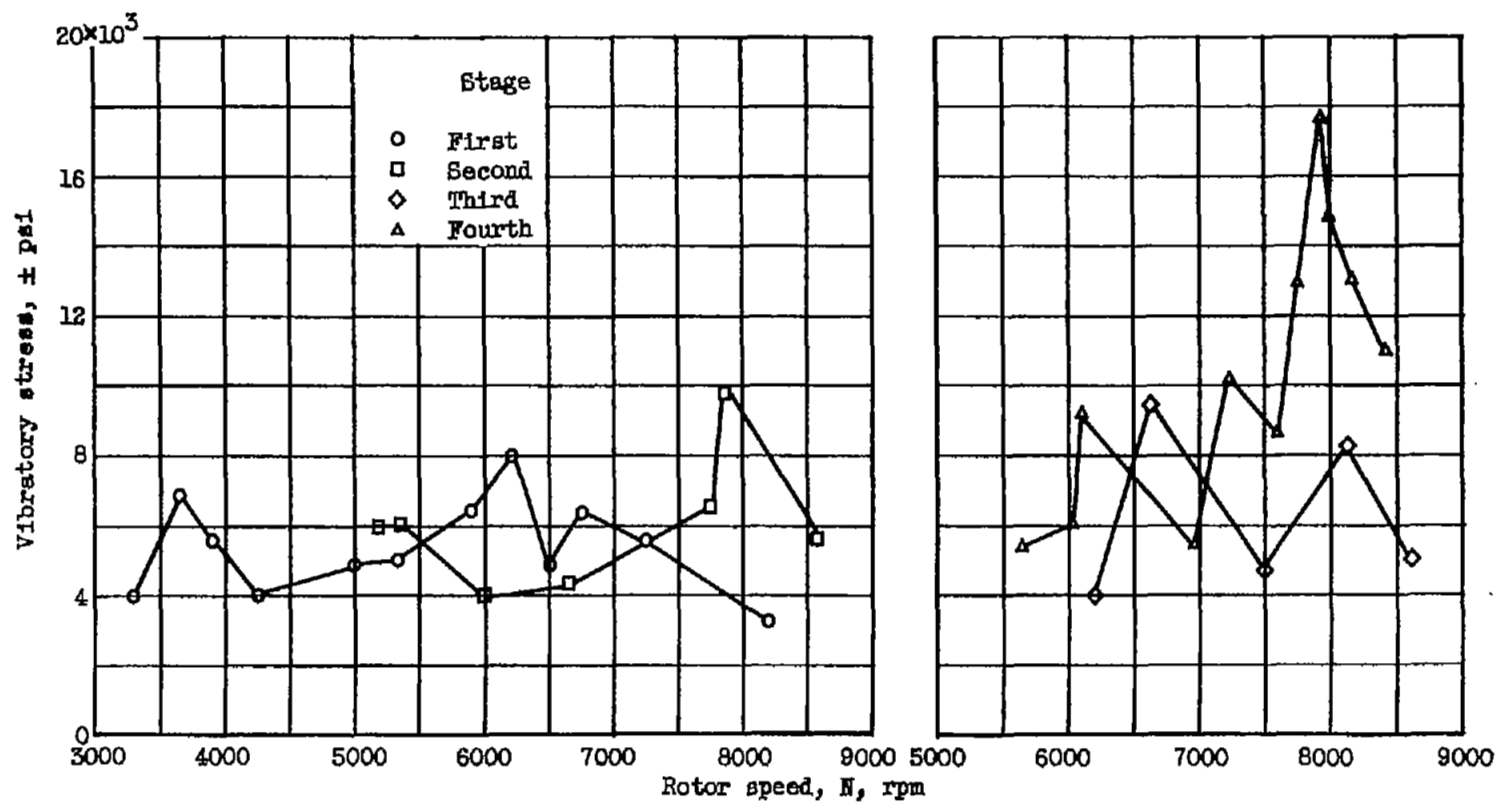on figure 10.

Figure 10. - Variation of rotor blade vibration with rotor speed.